Elsevier Editorial System(tm) for Cell Reports
Manuscript Draft

Manuscript Number: CELL-REPORTS-D-11-00090R2

Title: Rhythmic nucleotide synthesis in the liver: temporal segregation of metabolites.

Article Type: Report

Keywords: circadian; metabolome; purine; pyrimidine; nucleotide synthesis

Corresponding Author: Professor Hitoshi Okamura, M.D., Ph.D.

Corresponding Author's Institution: Kyoto University

First Author: Jean-Michel Fustin

Order of Authors: Jean-Michel Fustin; Masao Doi; Hiroyuki Yamada; Rie Komatsu; Shigeki Shimba; Hitoshi Okamura, M.D., Ph.D.

Abstract: The synthesis of nucleotides in the body is centrally controlled by the liver, via salvage or de novo synthesis. We reveal a pervasive circadian influence on hepatic nucleotide metabolism, from rhythmic gene expression of rate-limiting enzymes to oscillating nucleotide metabolome in WT mice. Genetic disruption of the hepatic clock leads to aberrant expression of these enzymes, together with anomalous nucleotide rhythms, such as constant low levels of ATP with an excess in uric acid, the degradation product of purines. These results clearly demonstrate that the hepatic circadian clock orchestrates nucleotide synthesis and degradation. This circadian metabolome time-table, obtained using state-of-the-art Capillary Electrophoresis Time-of-Flight Mass Spectrometry, will guide further investigations in nucleotide metabolism-related disorders.

Cover Letter

Dear Dr. Sabbi Lall, Scientific Editor for Cell Reports,

Thank you very much for your positive and encouraging letter. We were delighted by the reception our revisions received from you and the two reviewers.

We have of course modified the manuscript according to the two last comments made by the reviewers. The title has changed and does not include the word “metabolome”, and the discussion on page 5 has been slightly modified.

The character count of the manuscript is 33,858, slightly above the 32,000 limit. We hope it is acceptable, since we feel that excessive shortening of the manuscript would hamper the clear understanding of our message for non-specialists. Please let us know.

Thank you for your continued consideration,

Okamura Hitoshi
Kyoto University
Department of Systems Biology
Graduate School of Pharmaceutical Sciences
46-29 Yoshida-Shimo-Adachi-cho, Sakyo-ku,
Kyoto 606-8501, Japan
TEL : +81-75-753-9552
okamurah@pharm.kyoto-u.ac.jp

Response to reviewer's comments

Thanks you very much again for the encouragements you gave to our manuscript. We have of course changed it according to your justified comments.

For the reviewer #1:

-New title: "Rhythmic nucleotide synthesis in the liver: temporal segregation of metabolites." This title does not contain the word "metabolome" anymore. However, we felt that it needed a more specific statement in addition to simply "Rhythmic nucleotide synthesis in the liver". Therefore, we added the last part of the title, based on the cluster analysis data. We hope this is acceptable.

For the reviewer #2:

-Final paragraph on top of page 5 has been changed to: "Together these data suggest the rhythmic *de novo* synthesis is under predominant systemic control, but modulated by the local liver clock." We hope this will satisfy.

Graphical Abstract

Click here to download Graphical Abstract: graphical abstract.eps

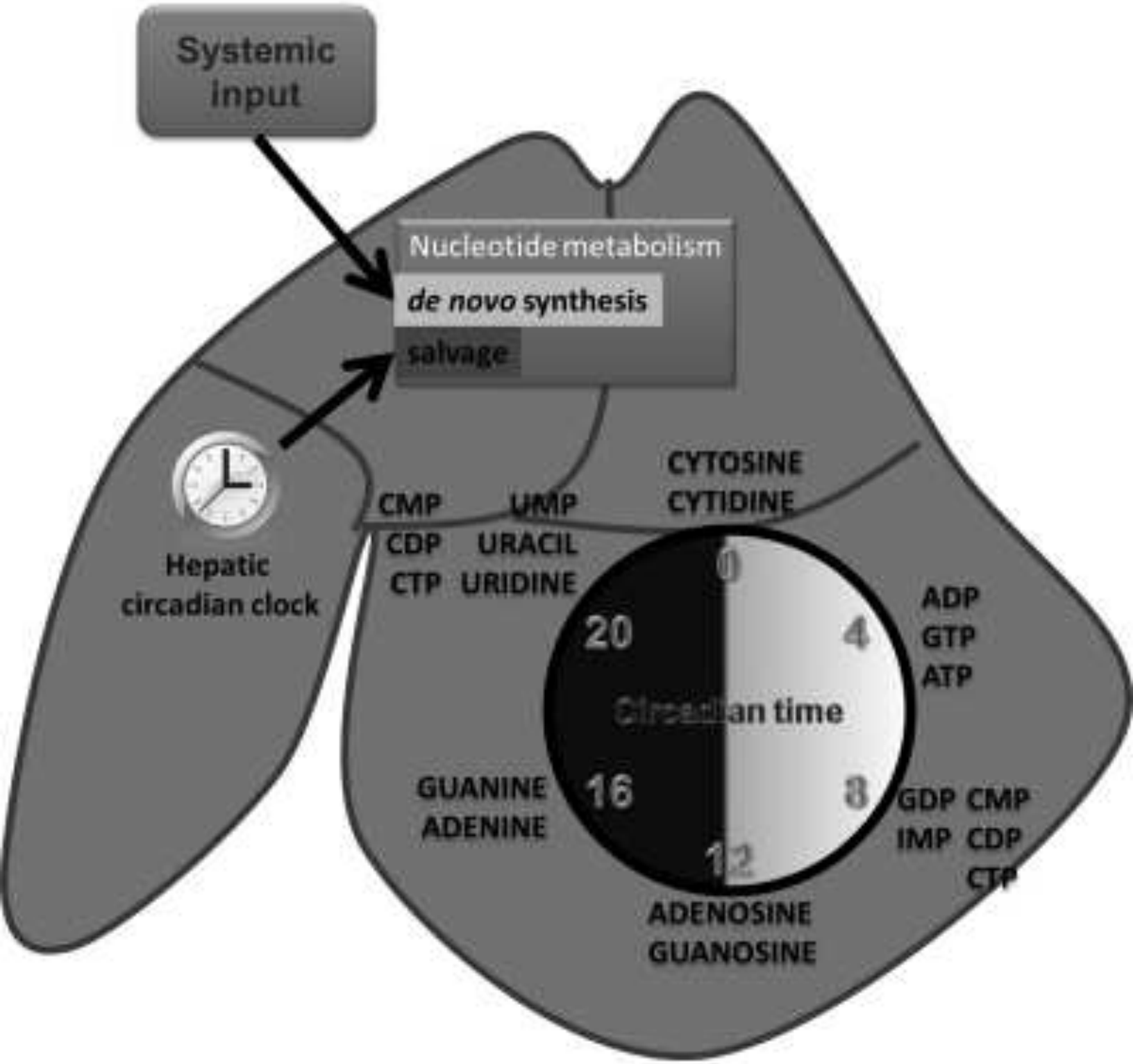

Highlights:

-Nucleotide synthesis and degradation is controlled by the hepatic clock.

-Loss of hepatic clock leads to low nucleotide abundance.

-Loss of hepatic clock leads to high uric acid levels.

Rhythmic nucleotide synthesis in the liver: temporal segregation of metabolites.

Jean-Michel Fustin[1], Masao Doi[1], Hiroyuki Yamada[1], Rie Komatsu[1], Shigeki Shimba[2], Hitoshi Okamura[1,3]

1: Kyoto University, Graduate School of Pharmaceutical Sciences, Department of System Biology, Graduate School of Pharmaceutical Sciences, 46-29 Yoshida-Shimo-Adachi-cho, Sakyo-ku, Kyoto, 606-8501, Japan.

2: Department of Health Science, College of Pharmacy, Nihon University, Funabashi, Chiba, 274-8555, Japan.

3: Corresponding author:

okamurah@pharm.kyoto-u.ac.jp

Fax: +81-(0)75-753-9553

Phone: +81-(0)75-753-9552

Summary

The synthesis of nucleotides in the body is centrally controlled by the liver, via salvage or *de novo* synthesis. We reveal a pervasive circadian influence on hepatic nucleotide metabolism, from rhythmic gene expression of rate-limiting enzymes to oscillating nucleotide metabolome in WT mice. Genetic disruption of the hepatic clock leads to aberrant expression of these enzymes, together with anomalous nucleotide rhythms, such as constant low levels of ATP with an excess in uric acid, the degradation product of purines. These results clearly demonstrate that the hepatic circadian clock orchestrates nucleotide synthesis and degradation. This circadian metabolome time-table, obtained using state-of-the-art Capillary Electrophoresis Time-of-Flight Mass Spectrometry, will guide further investigations in nucleotide metabolism-related disorders.

Introduction

The circadian clock synchronises physiology and behaviour to the appropriate time of day and endogenously generates rhythms under constant conditions. The clock regulates the transcription of thousands of target clock-controlled genes involved in fundamental metabolic pathways (Akhtar et al., 2002; Lamia et al., 2008; Panda et al., 2002; Reddy et al., 2006; Ueda et al., 2002; Vollmers et al., 2009), but the metabolic consequences of such regulation often remain to be described.

Two essential discoveries, the circadian control of the cell cycle (Matsuo et al., 2003) and DNA repair (Kang et al., 2010) in the liver, suggest the supply of nucleotides itself is regulated by the circadian clock. Since the liver is a site of active *de novo* nucleotide synthesis and controls the supply of free bases and nucleosides to other tissues for salvage (Barsotti et al., 2002; Cansev, 2006; Cao et al., 2005; Gasser et al., 1981), the circadian control of hepatic nucleotide metabolism will have wide implications for the body.

To define the role of the hepatic clock in the control of nucleotide metabolism, we analysed gene expression and metabolome of wild-type and liver *Bmal1*-deficient mice (*Bmal1*$^{L-/-}$), which show rhythmic activity and food intake but lack a functional molecular clock in the liver driving hepatic physiology (Shimba et al., 2011). We show that the expression of rate-limiting enzymes in nucleotide metabolism is under clock-control, and that nucleotides are rhythmic and time-segregated. In *Bmal1*$^{L-/-}$ liver, aberrant expression of these enzymes is correlated with the disruption of nucleotide rhythms. In particular, ATP and was constantly low and uric acid was increased, suggesting inefficient purine synthesis and/or increased degradation. We here provide the first integrated transcriptome and metabolome circadian timetable focussed on a single metabolic pathway, in order to give insights into the physiological importance of the local hepatic clock for nucleotide synthesis, relevant for cancer chemotherapy and for the treatment of nucleotide imbalance disorders such as gout.

Results

The expression of genes involved in purine and pyrimidine nucleotide metabolism (KEGG mmu00230 and 00240, initially screened for rhythmic expression in microarray dataset at http://circadian.salk.edu) was analysed by quantitative real-time PCR from WT liver samples dissected every 4 hours during 24 hours. To avoid external interferences on the endogenous circadian clock, mice were housed in constant dark (DD) conditions with food and water *ad libitum*. To investigate the role of the liver circadian clock in the control of nucleotide biosynthesis, gene expression was analysed in clock-less liver generated by liver-specific disruption of the clock gene *Bmal1* (Shimba et al., 2011). The loss of temporal hepatic organisation was confirmed by the absence of *Bmal1* transcript and the aberrant rhythms of clock gene expression (Supplemental figure 1). For the sake of clarity, we only report genes that showed significant variations of expression ($p<0.05$ in one-way ANOVA in WT). The results presented here are largely consistent with previous microarray datasets (Vollmers et al., 2009), but some genes showing very low-amplitude oscillations on microarray were not significant in our analysis.

Rate-limiting enzymes in *de novo* nucleotide synthesis

De novo synthesis of nucleotides, with multiple enzymatic steps mediated by different genes, leads to the synthesis of inosine monophosphate (IMP, Fig. 1A) or uridine monophosphate (UMP, Fig. 1B), precursors for other nucleotides. The rate-limiting enzymes in the *de novo* synthesis of IMP (*Ppat*) (Nelson et al., 2008) and UMP (*Cad* and *Umps*) (Traut, 2009; Traut and Jones, 1977), showed significant circadian rhythms of expression. In *Bmal1*$^{L-/-}$ liver, their expression was significantly affected (*Ppat* showing elevated levels) but still displayed a rhythmic component.

The *de novo* synthesis of CTP from UTP is mediated by two enzymes called CTP synthases. Two isoforms exist, *Ctps* (cytosolic) and *Ctps2* (mitochondrial), both mediating the rate-limiting step in the synthesis of cytidine nucleotides. *Ctps* expression was circadian but *Ctps2* showed significant bimodal variations. In *Bmal1*$^{L-/-}$ liver, both genes still displayed rhythmic expression with lower amplitude but with a two-fold increase in baseline.

Together these data suggest the rhythmic *de novo* synthesis is under predominant systemic control, but modulated by the local liver clock.

Mitochondrial nucleotide monophosphate kinases

The phosphorylation of nucleotide monophosphates, mediated by specific kinases, is a critical step towards the synthesis of NTPs (Nelson et al., 2008). Among these kinases, only the mitochondrial isoforms *Ak2*, *Ak4* (Fig.1A) and *Cmpk2* (Fig. 1B) showed significant rhythmic expressions. *Ak2* and *Ak4* showed identical waveforms in WT and were similarly affected in *Bmal1*$^{L-/-}$, showing lower expression with a bimodal pattern. *Cmpk2* in contrast showed higher expression in *Bmal1*$^{L-/-}$ but remained rhythmic. This suggests that the rhythmic supply of nucleotide diphosphate, ADP in particular, is important in the mitochondria where ATP is synthesised. Lower *Ak* expression but higher *Cmpk2* expression may cause an imbalance in purine/pyrimidine content.

dNDP synthesis is controlled by the circadian clock

Deoxynucleotide synthesis from nucleotide diphosphate is mediated by a single enzyme called ribonucleotide reductase M (RRM). RRM is composed of two subunits, RRM1 and RRM2 (Nelson et al., 2008), the latter being rate-limiting for the activity of the enzyme (Zuckerman et al., 2011). *Rrm1* expression in liver was constant; while *Rrm2* displayed pronounced circadian variations (Fig. 1 and Sup. figure 2B). Nadir *Rrm2* mRNA levels were three times lower than those of *Rrm1*, while at peak level they were equivalent, suggesting indeed a circadian control of

RRM activity via regulation of *Rrm2* expression. In *Bmal1*$^{L-/-}$ liver, *Rrm2* remained constantly low. This particular enzyme is interesting since it operates both on purines and pyrimidines, and since the synthesis of dNTPs is specifically for DNA replication and repair. Lower *Rrm2* expression in clock-less liver may cause dNTPs insufficiency and hamper liver regeneration after injury.

Nucleotide degradation and salvage

The degradation of nucleosides to free bases, an important step for their subsequent salvage by other tissues (Balestri et al., 2007; Griffiths and Stratford, 1997; Markert, 1991; Pizzorno et al., 2002), is mediated by nucleoside phosphorylases. All hepatic nucleoside phosphorylases showed significant and high-amplitude rhythmic expression: *Pnp* (Fig. 1A), *Tymp* and *Upp2* (Fig. 1B). *Pnp*, *Tymp* and *Upp2* were highly expressed in the liver compared to other tissues (Sup. figure 2A), but *Upp1* was barely detectable and was not significant (Sup. figure 2B). In addition, *Tk1* and *Tk2*, salvaging thymidine to dTMP in the cytoplasm and mitochondria respectively (Munch-Petersen, 2010), were rhythmically expressed in the liver (Fig. 1B).

In *Bmal1*$^{L-/-}$ liver, *Upp2* expression lost its peak at CT12 and showed a low bimodal pattern. *Tymp* and *Pnp* showed increased expression, but with a residual rhythm of lower amplitude. *Tk1* and *Tk2* were both significantly affected, showing higher baseline and bimodal expression.

Together these results suggest that the hepatic clock, together with systemic cues, orchestrate nucleotide synthesis and degradation. To test this hypothesis, we quantified circadian liver metabolome by Capillary Electrophoresis Time-of-Flight Mass Spectrometry (CE-TOFMS) in WT mice, every 4 hours during 24 hours.

Rhythmic abundance of bases, nucleosides and nucleotides by CE-TOFMS

CE-TOFMS analysis of liver metabolome revealed pervasive rhythms in free purine and pyrimidine bases, nucleosides and nucleotides (Fig. 2A and B).

The rhythms of IMP and UMP were similar to that of the expression of their own synthetic enzymes: *Ppat* and IMP rose during the day, *Cad* and *Umps* peaked at night with UMP.

The purine nucleotides ADP, ATP, GDP and GTP all had similar phases (Fig. 2A), which is consistent with the two parallel branches of the purine pathway. Since ATP allosterically regulates the synthesis of GMP from IMP, it is likely that the rhythm observed for ATP drives that of GTP. In contrast, all cytidine nucleotides showed significant bimodal patterns (Fig. 2B), very similar to *Ctps2* expression. In contrast, UDP and UTP did not show significant variations.

The purine bases adenine and guanine peaked at night, rising at the end of the day in a pattern similar to *Pnp* expression and in antiphase to adenosine and guanosine. Similarly, uridine abundance was antiphasic to *Upp2* expression. Due to efficient degradation of pyrimidine free bases to soluble metabolites in the liver, the uracil rhythm closely mirrored that of uridine an order of magnitude lower. Since no cytidine phosphorylase has so far been discovered in mammals, it is likely that the rhythms observed for cytidine and cytosine depend mostly on digestion. A similar rhythm in cytidine, peaking during the subjective day, was previously reported in a partial circadian metabolomics study from mouse plasma (Minami et al., 2009).

Hierarchical clustering by Pearson correlation (Fig. 2C) revealed that purines are time-segregated, with nucleotides peaking in the mid-subjective day, followed by nucleosides at CT12, then by the adenine and guanine bases at CT16. ATP and GTP originate from the two opposite branches of the purine pathway but are perfectly synchronous. Clearly, a tight regulation of purines operates, resulting in a constant ratio between ATP and GTP throughout the day. Adenosine nucleotides are the most abundant purines (Sup. figure 3A), reflecting their metabolic importance.

Hierarchical clustering of pyrimidines revealed a different pattern (Fig. 2D). Here, the highest level of temporal organisation reflected the nature of the base used, either uracil or cytosine.

This underlines the differences between the two parallel and symmetric branches of the purine pathway versus the asymmetric and serial pyrimidine pathway (compare Fig. 1A and B). The most abundant pyrimidine is UMP, consistent with it being the precursor for all other pyrimidine nucleotides (Supplemental figure 3B).

Similar to the disrupted rhythmic expression of genes presented in Fig. 1, we predict that the nucleotide rhythms presented here will likewise be affected by the loss of the hepatic clock.

Loss of liver clock affects nucleotide rhythms and abundance

To determine which nucleotide rhythms and abundance are affected by the loss of the hepatic clock, we compared the nucleotide metabolome of *Bmal1*$^{L-/-}$ and *Bmal1*$^{f/f}$ mice at CT4 and CT16. These time points were chosen since they often correspond to high and low nucleotide abundance in WT mice. We present the results of this analysis organised in a metabolic map, similar to that used in Fig. 1.

IMP and UMP were little affected by the loss of the liver clock. While circadian time had a strongly significant effect on the abundance of both, only UMP showed a significant time/genotype interaction in two-way ANOVA. This is reminiscent of *Ppat*, *Cad* and *Umps* expression in Fig. 1: while they were affected by the loss of the hepatic clock, a rhythmic expression persisted, suggesting systemic control of *de novo* nucleotide synthesis by rhythmic cues.

AMP significantly increased in *Bmal1*$^{L-/-}$ liver but ATP remained low, which is consistent with the blunted expression pattern of *Ak2* and *Ak4*, resulting in a lower ADP/AMP ratio. The opposite branch of the purine pathway appeared similarly but somewhat less affected. GTP showed blunted CT4/CT16 fold ratio (genotype/time interaction significantly different in two way ANOVA, $p<0.05$). Together this is consistent with a primary circadian regulation of ATP synthesis that in turn drives changes in GTP via allosteric control.

For pyrimidines, UTP and UDP were significantly lower in *Bmal1*$^{L-/-}$ liver, despite showing non-significant circadian variations in WT mice. CTP and CMP levels at CT4 were similar between genotypes, but at CT16 they increased in *Bmal1*$^{L-/-}$ liver while they decreased in WT, suggesting altered phase of synthesis, with higher basal synthesis level in clock-less liver.

The purine nucleosides adenosine and guanosine were less abundant in *Bmal1*$^{L-/-}$ liver, but showed CT4/CT16 variations as in WT. Adenine base however showed a reduction in the CT4/CT16 fold ratio. Low adenosine and blunted adenine rhythm are consistent with higher expression levels but lower amplitude rhythm observed for *Pnp* in Fig. 1. For pyrimidine nucleosides, uridine showed increased levels in *Bmal1*$^{L-/-}$ liver, but cytidine was not affected.

Interestingly, the degradation product of purine nucleotides, uric acid, whose excess in human leads to gout, was elevated in *Bmal1*$^{L-/-}$ liver, suggesting indeed that the balance between synthesis (low ATP levels) and degradation (high urate) of purines is tilted towards degradation.

Together these data provide direct evidence that the hepatic circadian clock orchestrates the entire nucleotide metabolic pathway, in synchrony with systemic cues.

Discussion

Nucleotide metabolism within the liver is orchestrated by the hepatic circadian clock but also synchronised at the level of the whole organism. Firstly, *de novo* synthesis appears to respond mostly to systemic signals, which is consistent with the restricted feeding/fasting-driven rhythmic expression of *Ppat*, *Umps* and *Cad* in clock-deficient animal reported in a previous dataset (Vollmers et al., 2009). Secondly, the degradation of all nucleosides to their respective free bases appears regulated by the hepatic clock via control of phosphorylases transcription, but the rhythmic abundance of nucleosides likely reflects their absorption from food. Indeed, all nucleoside variations between CT4 and CT16 show parallel changes in WT and clock-deficient liver. Taken together, systemic and local circadian regulation of nucleotide metabolism will

regulate the amount of free bases and/or nucleosides released into the circulation for salvage, while ensuring an appropriately timed flow of newly synthesised nucleotides into the hepatic pool. This is especially obvious for purines, since all rhythmic genes involved in the anabolism of purines (*Ppat, Ak2, Ak4 and Rrm2*) show synchronized expression with a peak around CT12, in contrast to *Pnp* peaking at CT20.

The influence of the hepatic clock is mostly seen in the phosphorylation of nucleotides. All nucleotide triphosphates synthesised from their monophosphate forms (ATP, GTP, UTP) show lower abundance and/or amplitude in clock-less liver. The blunted *Ak2* and *Ak4* expression in *Bmal1*$^{L-/-}$ liver is consistent with these observations for ATP and GTP. UTP was not rhythmic in WT but its decreased abundance in *Bmal1*$^{L-/-}$ liver clearly indicates nucleotide synthesis as a whole suffers from the loss of the hepatic clock. The same is true for opposite variations of cytidine nucleotides.

The expression rhythms of mitochondrial kinases (*Ak2*, *Ak4*, *Cmpk2* and *Tk2*) suggest that timed nucleotide conversion is especially important in mitochondria, perhaps because they rely exclusively on nucleotide salvage and have a more dynamic genome (Rotig and Poulton, 2009). Notably, AKs are critically important in the control of cellular energy homeostasis, by regulating the amount of ADP available for the synthesis of ATP (Noma, 2005), 70% of which originate from mitochondria. We propose that the constant low levels in *Ak2* and *Ak4* expression may contribute to decreased supply of ADP, in turn leading to low ATP levels, affecting in turn the synthesis of other nucleotides. Similarly, overexpression of both *Ctps* and *Ctps2* in *Bmal1*$^{L-/-}$ liver is likely to contribute to lower UTP and higher CTP and CMP levels observed in these animals.

Available data on the *Arabidopsis* circadian transcriptome (Mockler et al., 2007) reveals that plant homologues of *Rrm2*, *Ak*, *Ppat* and *Cad* show a circadian component in their expression. Interestingly, most of these homologues are targeted to chloroplasts or mitochondria, where the

de novo synthesis of nucleotides in plant is located (Zrenner et al., 2006). The evolutionary conserved circadian nucleotide synthesis, located in different subcellular compartments, essentially times maximal availability of nucleotides when they are required the most. As a concrete example in mammals, nucleotide excision repair activity in adult mouse liver and brain DNA is maximal at CT12 (Kang et al., 2009; Kang et al., 2010), when *Rrm2* expression is highest, replenishing the pool of dNTPs.

AMP-activated protein kinase (AMPK), whose activity is allosterically regulated by the AMP/ATP ratio, was found to regulate the circadian clock (Lamia et al., 2009). Interestingly, the AMP/ATP ratio will change during the day due to constant AMP levels but cyclic ATP abundance. The circadian clock thus regulates ATP levels, which may in turn feedback to adjust the clock in a complex interplay between metabolism and the clock, the topic of recent reviews (Asher and Schibler, 2011; Bass and Takahashi, 2010; Schmutz et al., 2011). The role of adenylate kinases, more precisely of *Ak2*, in the generation of circadian rhythms has even been suggested previously (Noma, 2005). To confirm the rhythmic expression of AK2, the variations of its protein in the liver are shown in Sup. fig. 4.

An important question that has not been addressed in our study is whether the disruption of nucleotide rhythms and abundance leads to pathologies in *Bmal1*$^{L-/-}$ animals. The increased uric acid observed in *Bmal1*$^{L-/-}$ liver, despite its efficient degradation in mouse liver (as opposed to human in which UOX, the enzyme oxidising urate, is a pseudogene), may have pathological consequences under special circumstances. In addition, the regenerating liver, as well as peripheral tissues with high proliferative rates such as bone marrow or thymus, may be adversely affected due to nucleotide imbalances seen in the liver of *Bmal1*$^{L-/-}$ animals. Further investigations will address these possibilities.

Conclusions.

Hepatic nucleotide metabolism is timely orchestrated, from the transcriptional control of rate-limiting genes to the rhythmic abundance of metabolites. The loss of the local hepatic circadian clock causes significant perturbations in the normal rhythms of nucleotides likely affecting the physiology of the whole animal. These results represent a novel integrative approach, linking transcriptomics with high-end metabolomics, focussing on the circadian control of a well characterised metabolic pathway.

Experimental Procedures

Animals. All experiments were approved by the animal experimentation committee of Kyoto University. Liver specific *Bmal1*-deficient mice on a full C57BL/6J background (*Bmal1*$^{L-/-}$) and *Bmal1*$^{f/f}$ were generated as described (Shimba et al., 2011). Male C57BL/6J mice and *Bmal1*$^{L-/-}$ mice (8 weeks old) were maintained at 23 ± 1°C with 50 ± 10% relative humidity, three animals per cage on a 12 h light/12 h dark cycle (lights on 8:00, lights off 20:00), food and water *ad libitum*. At the end of the last dark phase, light was permanently switched off. On the second day in DD, starting from CT0 (CT0 beginning of the endogenous day, CT12 beginning of the endogenous night, 8:00 and 20:00 respectively), animals (n=3) were sacrificed every four hours under a safe red light and sampled for liver RNA extraction and metabolomics analysis.

RNA extraction and quantitative real-time PCR. Mice were sacrificed by cervical dislocation and 50 mg from the left liver lobe were immediately transferred in 1ml Trizol (Invitrogen, Tokyo, Japan) and homogenised using TissueLyzer (Qiagen, Tokyo, Japan). Homogenates were processed for total RNA extraction (RNeasy, Qiagen), and final RNA samples were quantified by Nanodrop spectrophotometer. 1.5 μg total RNA from each liver sample was reverse-transcribed using VILO (Invitrogen). Quantitative real-time PCR was performed on 20 ng cDNA using Platinum SYBR Green qPCR Supermix (Invitrogen) in StepOnePlus (Applied Biosystems, Tokyo, Japan). Absolute quantification standards for each target cDNA were obtained using band-purified PCR products as templates, synthesised using the same primer pairs used in qPCR and verified by sequencing (see primer list in supplemental table 1). All PCR products used for standard and quantification were of similar sizes (120-150 bp) and molecular weight (~40 KDa). Data were then normalised using relative expression of the housekeeping gene *Tbp*.

CE-TOFMS. At the time of liver sample collection for qPCR, another 50mg sample from the left liver lobe, adjacent to the fragment previously taken, was excised and immediately transferred to a 2 ml tube, then snap-frozen in liquid nitrogen. All samples were kept a few days at -80°C until analysis. Samples were then sent for CE-TOFMS analysis to Human Metabolome Technologies (Tokyo, Japan)**.** See supplemental materials for additional information.

Statistical analyses. Gene expression and metabolites concentration in wild-type mice were analysed by One-way ANOVA. To compare *Bmal1*$^{L-/-}$ and WT mice, gene expression profiles were tested by Two-way ANOVA. All statistical analyses were performed using Graphpad Prism 4.0. For hierarchical clustering analysis of liver metabolites, raw concentration data of circadian metabolites were normalised and mean centred, and then clustered by Pearson Correlation Coefficients (Eisen et al., 1998). This was performed using GenePattern available from The Broad Institute.

Financial Support

This work was supported by Specially Promoted Research (to H.O.), and a scientific grant and the "High-Tech Research Center" Project for Private Universities, a matching fund subsidy (to S.S.) from the Ministry of Education, Culture, Sports, Science and Technology of Japan, and grants from the Health Labour Sciences Research of Japan, SRF, Takeda Science Foundation (to H.O). J.-M.F. is supported by a JSPS Postdoctoral Fellowship Program (Short-term) for North American and European Researchers, a JSPS Postdoctoral Fellowship Program for Foreign Researchers and a Takeda Science Foundation research fellowship.

References

Akhtar, R.A., Reddy, A.B., Maywood, E.S., Clayton, J.D., King, V.M., Smith, A.G., Gant, T.W., Hastings, M.H., and Kyriacou, C.P. (2002). Circadian cycling of the mouse liver transcriptome, as revealed by cDNA microarray, is driven by the suprachiasmatic nucleus. Curr. Biol. *12,* 540-550.

Asher, G., and Schibler, U. (2011). Crosstalk between components of circadian and metabolic cycles in mammals. Cell. Metab. *13,* 125-137.

Balestri, F., Barsotti, C., Lutzemberger, L., Camici, M., and Ipata, P.L. (2007). Key role of uridine kinase and uridine phosphorylase in the homeostatic regulation of purine and pyrimidine salvage in brain. Neurochem. Int. *51,* 517-523.

Barsotti, C., Tozzi, M.G., and Ipata, P.L. (2002). Purine and pyrimidine salvage in whole rat brain. Utilization of ATP-derived ribose-1-phosphate and 5-phosphoribosyl-1-pyrophosphate generated in experiments with dialyzed cell-free extracts. J. Biol. Chem. *277,* 9865-9869.

Bass, J., and Takahashi, J.S. (2010). Circadian integration of metabolism and energetics. Science *330,* 1349-1354.

Cansev, M. (2006). Uridine and cytidine in the brain: their transport and utilization. Brain Res. Rev. *52,* 389-397.

Cao, D., Leffert, J.J., McCabe, J., Kim, B., and Pizzorno, G. (2005). Abnormalities in uridine homeostatic regulation and pyrimidine nucleotide metabolism as a consequence of the deletion of the uridine phosphorylase gene. J. Biol. Chem. *280,* 21169-21175.

Eisen, M.B., Spellman, P.T., Brown, P.O., and Botstein, D. (1998). Cluster analysis and display of genome-wide expression patterns. Proc. Natl. Acad. Sci. U. S. A. *95,* 14863-14868.

Gasser, T., Moyer, J.D., and Handschumacher, R.E. (1981). Novel single-pass exchange of circulating uridine in rat liver. Science *213,* 777-778.

Griffiths, L., and Stratford, I.J. (1997). Platelet-derived endothelial cell growth factor thymidine phosphorylase in tumour growth and response to therapy. Br. J. Cancer *76,* 689-693.

Kang, T.H., Lindsey-Boltz, L.A., Reardon, J.T., and Sancar, A. (2010). Circadian control of XPA and excision repair of cisplatin-DNA damage by cryptochrome and HERC2 ubiquitin ligase. Proc. Natl. Acad. Sci. U. S. A. *107,* 4890-4895.

Kang, T.H., Reardon, J.T., Kemp, M., and Sancar, A. (2009). Circadian oscillation of nucleotide excision repair in mammalian brain. Proc. Natl. Acad. Sci. U. S. A. *106,* 2864-2867.

Lamia, K.A., Sachdeva, U.M., DiTacchio, L., Williams, E.C., Alvarez, J.G., Egan, D.F., Vasquez, D.S., Juguilon, H., Panda, S., Shaw, R.J., Thompson, C.B., and Evans, R.M. (2009). AMPK regulates the circadian clock by cryptochrome phosphorylation and degradation. Science *326,* 437-440.

Lamia, K.A., Storch, K.F., and Weitz, C.J. (2008). Physiological significance of a peripheral tissue circadian clock. Proc. Natl. Acad. Sci. U. S. A. *105,* 15172-15177.

Markert, M.L. (1991). Purine nucleoside phosphorylase deficiency. Immunodefic. Rev. *3,* 45-81.

Matsuo, T., Yamaguchi, S., Mitsui, S., Emi, A., Shimoda, F., and Okamura, H. (2003). Control mechanism of the circadian clock for timing of cell division in vivo. Science *302,* 255-259.

Minami, Y., Kasukawa, T., Kakazu, Y., Iigo, M., Sugimoto, M., Ikeda, S., Yasui, A., van der Horst, G.T., Soga, T., and Ueda, H.R. (2009). Measurement of internal body time by blood metabolomics. Proc. Natl. Acad. Sci. U. S. A. *106,* 9890-9895.

Mockler, T.C., Michael, T.P., Priest, H.D., Shen, R., Sullivan, C.M., Givan, S.A., McEntee, C., Kay, S.A., and Chory, J. (2007). The DIURNAL project: DIURNAL and circadian expression profiling, model-based pattern matching, and promoter analysis. Cold Spring Harb. Symp. Quant. Biol. *72,* 353-363.

Munch-Petersen, B. (2010). Enzymatic regulation of cytosolic thymidine kinase 1 and mitochondrial thymidine kinase 2: a mini review. Nucleosides Nucleotides Nucleic Acids *29,* 363-369.

Nelson, D.L., Cox, M.M., Lehninger, A.L., and Lehninger, A.L. (2008). Lehninger principles of biochemistry (New York: Freeman).

Noma, T. (2005). Dynamics of nucleotide metabolism as a supporter of life phenomena. J. Med. Invest. *52,* 127-136.

Panda, S., Antoch, M.P., Miller, B.H., Su, A.I., Schook, A.B., Straume, M., Schultz, P.G., Kay, S.A., Takahashi, J.S., and Hogenesch, J.B. (2002). Coordinated transcription of key pathways in the mouse by the circadian clock. Cell *109,* 307-320.

Pizzorno, G., Cao, D., Leffert, J.J., Russell, R.L., Zhang, D., and Handschumacher, R.E. (2002). Homeostatic control of uridine and the role of uridine phosphorylase: a biological and clinical update. Biochim. Biophys. Acta *1587,* 133-144.

Reddy, A.B., Karp, N.A., Maywood, E.S., Sage, E.A., Deery, M., O'Neill, J.S., Wong, G.K., Chesham, J., Odell, M., Lilley, K.S., Kyriacou, C.P., and Hastings, M.H. (2006). Circadian orchestration of the hepatic proteome. Curr. Biol. *16,* 1107-1115.

Rotig, A., and Poulton, J. (2009). Genetic causes of mitochondrial DNA depletion in humans. Biochim. Biophys. Acta *1792,* 1103-1108.

Schmutz, I., Albrecht, U., and Ripperger, J.A. (2011). The role of clock genes and rhythmicity in the liver. Mol. Cell. Endocrinol.

Shimba, S., Ogawa, T., Hitosugi, S., Ichihashi, Y., Nakadaira, Y., Kobayashi, M., Tezuka, M., Kosuge, Y., Ishige, K., Ito, Y., *et al.* (2011). Deficient of a clock gene, brain and muscle Arnt-like protein-1 (*BMAL1*), induces dyslipidemia and ectopic fat formation. PLoS One *6,* e25231.

Traut, T. (2009). Nucleotide Synthesis *De Novo*. In eLS. John Wiley & Sons Ltd, Chichester.)

Traut, T.W., and Jones, M.E. (1977). Inhibitors of orotate phosphoribosyl-transferase and orotidine-5'-phosphate decarboxylase from mouse Ehrlich ascites cells: a procedure for analyzing the inhibition of a multi-enzyme complex. Biochem. Pharmacol. *26,* 2291-2296.

Ueda, H.R., Chen, W., Adachi, A., Wakamatsu, H., Hayashi, S., Takasugi, T., Nagano, M., Nakahama, K., Suzuki, Y., Sugano, S., *et al.* (2002). A transcription factor response element for gene expression during circadian night. Nature *418,* 534-539.

Vollmers, C., Gill, S., DiTacchio, L., Pulivarthy, S.R., Le, H.D., and Panda, S. (2009). Time of feeding and the intrinsic circadian clock drive rhythms in hepatic gene expression. Proc. Natl. Acad. Sci. U. S. A. *106,* 21453-21458.

Zrenner, R., Stitt, M., Sonnewald, U., and Boldt, R. (2006). Pyrimidine and purine biosynthesis and degradation in plants. Annu. Rev. Plant. Biol. *57,* 805-836.

Zuckerman, J.E., Hsueh, T., Koya, R.C., Davis, M.E., and Ribas, A. (2011). siRNA knockdown of ribonucleotide reductase inhibits melanoma cell line proliferation alone or synergistically with temozolomide. J. Invest. Dermatol. *131*, 453-460.

Figure Legends

Fig. 1. Rate-limiting enzymes are under transcriptional control by the hepatic circadian clock. Gene expression analysis in C57BL/6J and *Bmal1*$^{L-/-}$ mice, on the second day in constant darkness, starting from CT0 (n=3 mice per time points, sampled every 4 hours). One-way ANOVA was used to analyse gene expression profiles in WT mice, with significance levels given under the legend of each graph. Comparison of gene expression in the liver of C57BL/6J and *Bmal1*$^{L-/-}$ mice was performed by Two-way ANOVA, the significance levels are given under the title of each graph in the following order: interaction/genotype/time with * = $p<0.05$; ** = $p<0.01$; *** = $p<0.001$. The empty and filled rectangles over the X axis indicate subjective day and night, respectively. For visual clarity, data at CT0 is double plotted at CT24 in all graphs. (**A)**, Gene expression analysis of enzymes in the purine pathway. A simplified purine metabolic pathway is shown in the centre. Note the similar peak times for *Ppat*, *Rrm2*, *Ak2* and *Ak4*, different from that of *Pnp*. (**B)**, Gene expression analysis of enzymes in the pyrimidine pathway. A simplified pyrimidine metabolic pathway is shown in the centre. Green arrows indicate *de novo* synthesis (multiple enzymatic steps, but rate-limiting enzymes are indicated by a green label); blue, NMP kinases; red, NDP reductase; purple, nucleoside phosphorylases. Double black lines represent enzymatic activities encoded by non-rhythmic genes. All data presented are Mean +/- SEM.

Fig. 2. Rhythmic abundance of free bases, nucleosides and nucleotides in the liver. Quantification of purine and pyrimidine nucleotides, nucleosides and free bases in the liver of C57BL/6J mice sampled on the second day in constant darkness from CT0 (n= 3 animals per time point). Significance levels in One-way ANOVA are given on the upper right corner of each graph. The empty and filled rectangles over the X axis indicate subjective day and night, respectively. Here, the colour of curves indicate initial nucleotide monophosphate from the *de*

novo pathway (green), NDP and NTP (blue) and free bases and nucleosides (purple), corresponding to the colours used for the enzyme activities contributing to the regulation of these metabolites. For visual clarity, data at CT0 is double plotted at CT24 in all graphs. All data presented are Mean +/- SEM. **(A)**, Rhythmic profiles of purine nucleotides, nucleosides and free bases. **(B)**, Rhythmic profiles of pyrimidine nucleotides, nucleosides and free bases. **(C)**, Hierarchical clustering of purines using Pearson correlation coefficient displayed as a heat map. Note the clear clustering between nucleotides, nucleosides and free bases, forming three separated time-domains of maximal abundance. **(D)**, Hierarchical clustering of pyrimidines using Pearson correlation coefficient displayed as a heat map. Note here the clear higher-order clustering between cytidine nucleotides, nucleoside and bases; and UMP, uridine and uracil. All data presented are Mean +/- SEM.

Fig. 3. Loss of liver clock affects nucleotide rhythms and abundance. Absolute quantification of nucleotides, nucleosides and free bases in *Bmal1*$^{L-/-}$ and *Bmal1*$^{f/f}$ (WT) mice by CE-TOFMS at CT4 and CT16 (n=2). **(A)**, Purine pathway. Note IMP rhythm persists in *Bmal1*$^{L-/-}$ liver while ATP remains low. **(B)**, Pyrimidine pathway. Note opposite changes in UTP and CTP. Data were analysed by Two-way ANOVA. Significance levels in Two-way ANOVA are given under the title of each graph in the following order: interaction/genotype/time, with * = $p<0.05$; ** = $p<0.01$; *** = $p<0.001$. All data presented are Mean +/- SD.

Figure 1

Click here to download high resolution image

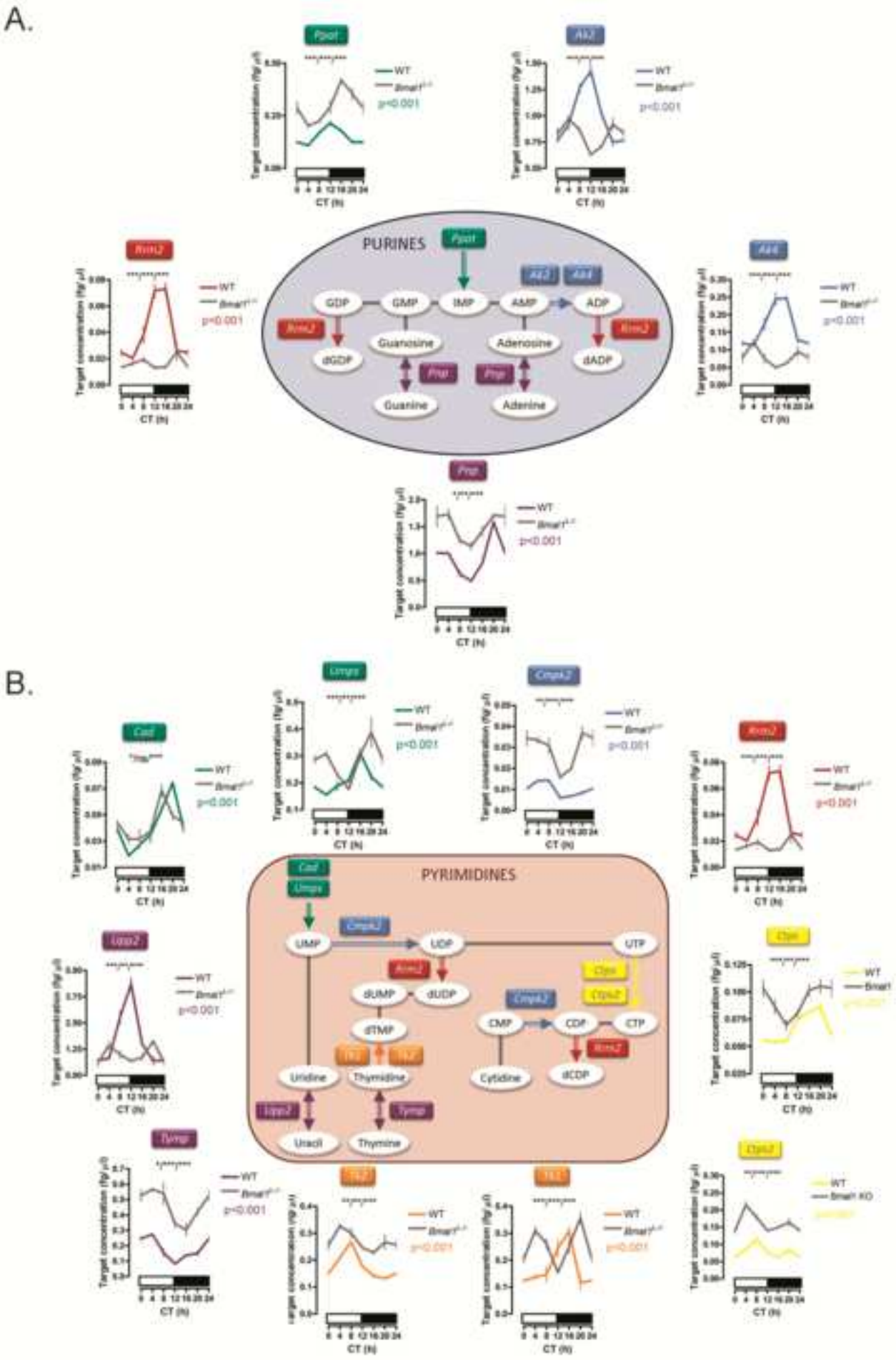

Figure 2

Click here to download high resolution image

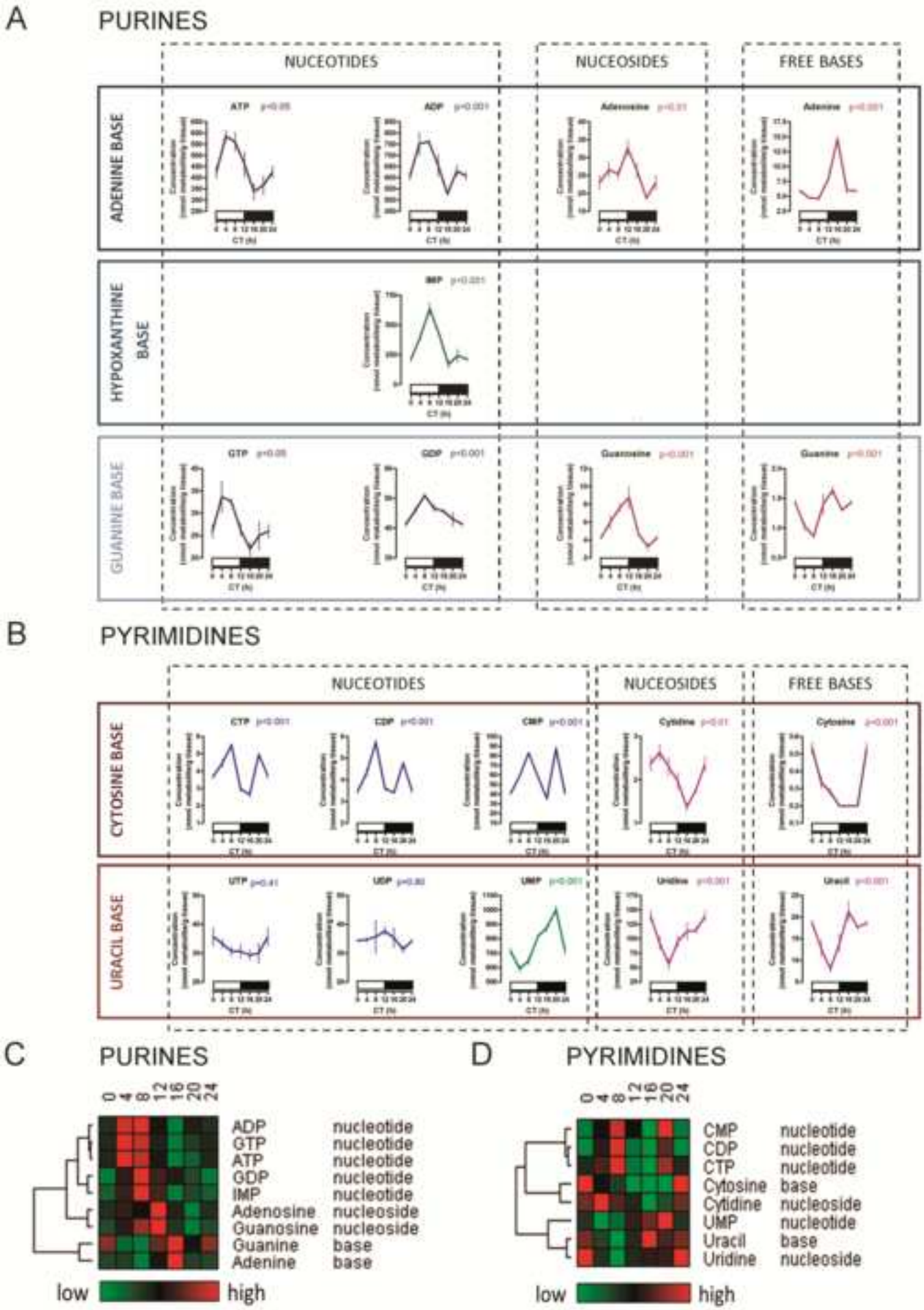

Figure 3

Click here to download high resolution image

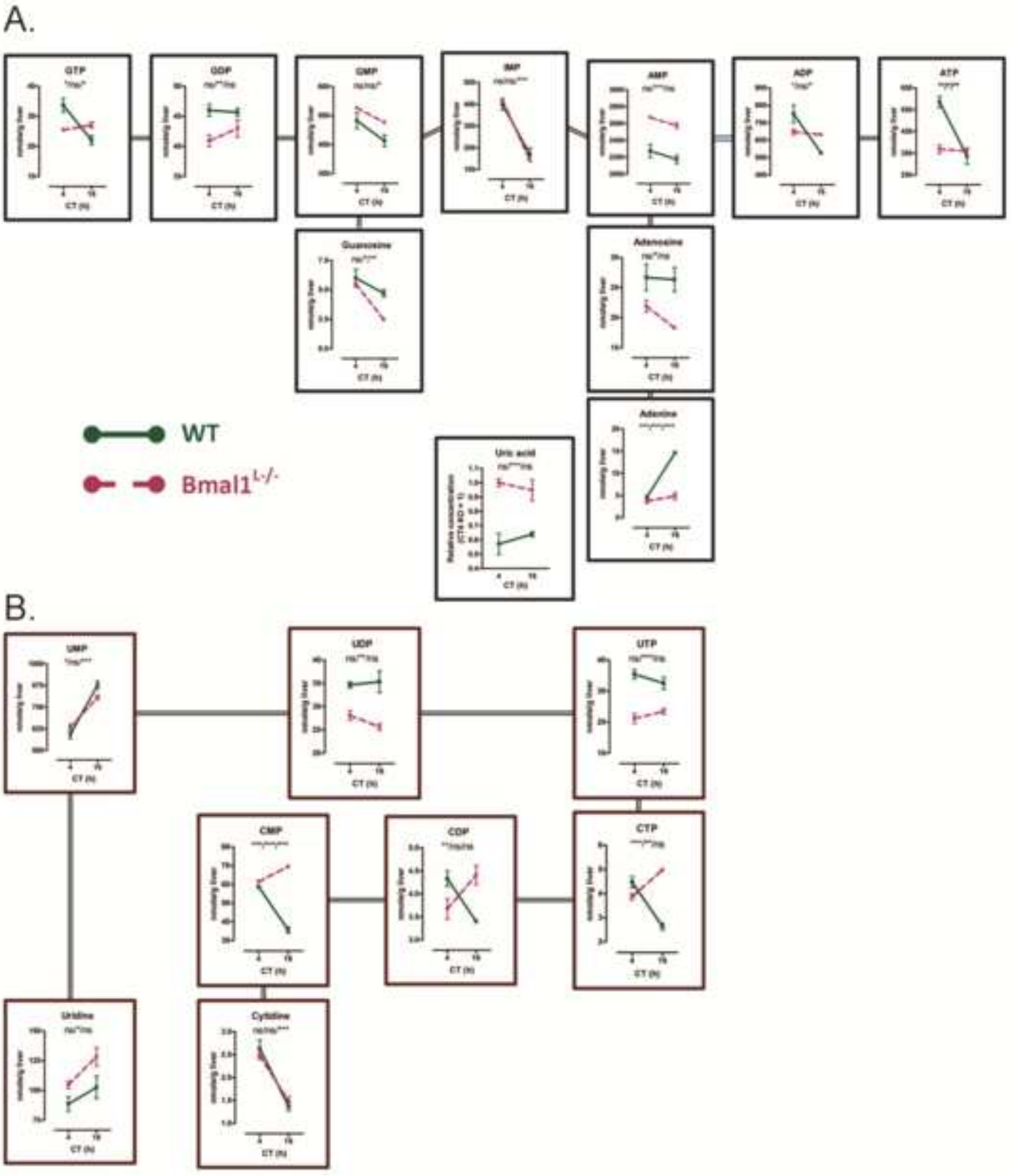

Supplemental Information Inventory

-A detailed explanation of the Capillary Electrophoresis Time-Of-Flight Mass-Spectrometry method employed. It is related to the data presented in Figure 2.

-A description of Western Blot method employed for the data of Supplemental Figure 4, which supports the data presented in Figure 1.

-Supplemental Figures:

- Supplemental Figure 1. *Bmal1*$^{L-/-}$ mice have disrupted circadian clock in the liver, related to Figure 1. Confirms the disruption of liver *Bmal1* expression.

- Supplemental Figure 2. Genes involved in the synthesis and supply of nucleotides are strongly expressed in the liver, related to Figure 1. Shows liver-specific expression of genes involved in nucleotide metabolism, supporting Figure 1-associated discussion.

- Supplemental Figure 3. Mean abundance of purine and pyrimidine in the liver, related to Figure 2. Shows mean abundance of nucleotides in the liver, supporting Figure 2.

- Supplemental Figure 4. Variations in AK2 protein quantity in the WT liver across a day in constant darkness, related to Figure 1. Shows Ak2 expression in the liver of WT mice, supporting Figure 1.

-Supplemental Table 1: shows the sequence of primers used for real-time PCR data presented in Figure 1.

-Supplemental References: related to the references cited in the extended methods pertaining to the CE-TOFMS.

Extended experimental procedures

CE-TOFMS. Frozen liver samples were homogenized (MS-100R; TOMY, Tokyo, Japan) in 500 ml of methanol. The homogenate was mixed with chloroform and Milli-Q water, and then centrifuged at 2,300 g for 5 min at 4℃. Subsequently, the aqueous phase was centrifuged at 9,100 g for 120 min at 4℃ for ultra-filtration through a 5 KDa filter (Millipore, Tokyo, Japan) to remove proteins. The filtrate was evaporated and dissolved in 50 μL of Milli-Q water for CE-TOFMS analysis. CE-TOFMS was carried out using an Agilent CE Capillary Electrophoresis System equipped with an Agilent 6210 Time of Flight mass spectrometer, Agilent 1100 isocratic HPLC pump, Agilent G1603A CE-MS adapter kit, and Agilent G1607A CE-ESI-MS sprayer kit (Agilent Technologies,Waldbronn, Germany). Metabolite peaks were compared to a reference standards database held in Human Metabolome Technologies.

The system was controlled by Agilent G2201AA ChemStation software version B.03.01 for CE (Agilent Technologies, Waldbronn, Germany). Cationic metabolites were analyzed with a fused silica capillary (50 μm i.d. × 80 cm total length), with Cation Buffer Solution (Human Metabolome Technologies) as the electrolyte and methionine sulfone as internal standard. The sample was injected at a pressure of 50 mbar for 10 sec (approximately 10 nl). The applied voltage was set at 27 kV. Electrospray ionization-mass spectrometry (ESI-MS) was conducted in the positive ion mode, and the capillary voltage was set at 4,000 V. The spectrometer was scanned from m/z 50 to 1,000. Other conditions were as in the cation analysis (Soga and Heiger, 2000).

Anionic metabolites were analyzed with a fused silica capillary (50 μm i.d. × 80 cm total length), with Anion Buffer Solution (Human Metabolome Technologies) as the electrolyte and PIPES as internal standard. The sample was injected at a pressure of 50 mbar for 25 sec (approximately 25 nl). The applied voltage was set at 30 kV. ESI-MS was conducted in the negative ion mode, and the capillary voltage was set at 3,500 V. The spectrometer was scanned from **m/z** 50 to 1,000. Other conditions were as in the anion analysis (Soga et al., 2007). Raw data obtained by CE-TOFMS were processed with the automatic

integration software MasterHands (Sugimoto et al., 2010). Peak information including m/z, migration time (MT) and area was obtained. Peak area was converted into relative peak area according to the equation: Relative peak area=Metabolite Peak Area/(Internal Standard Peak Area × Sample Amount). Each peak was aligned according to similar migration time on CE and m/z value determined by TOFMS. Near 100 metabolites were identified using this procedure.

Western Blot. Equivalent amounts of liver tissue (~50 mg) were dissected (n=2 animals per time points at CT 0, 4, 8, 12, 16 and 20) and homogenised in 0.5 ml RIPA buffer with a Dounce homogeniser. Homogenates were transferred to a 1.5 ml microtube and incubated at 4°C for 20 min, then centrifuged at 12,000 xg at 4°C for 15 min. The supernatant was aliquoted into new tubes. Protein homogenates were mixed with 5x Laemmli buffer, boiled at 95°C for 10 min, centrifuged for 5 min at 12,000 xg, then equivalent amounts of proteins (~ 10 μg in 15 μl) were loaded into each well. Samples were then run on a standard Polyacrylamide gel (ATTO pre-cast gel, 12.5%) at 25 mA for 20 min, then at 35 mA for 40 min in SDS TRIS-glycine buffer. Samples were then semi-dry blotted onto a PVDF membrane (ATTO, Japan) following manufacturer's protocol. Membrane was blocked with Blocking One (Nacalai Tesque, Japan) for 30 min at RT, then simultaneously incubated with anti-AK2 (ProteinTech, 11014-1-AP, x2000) and anti-β-actin (Sigma, A3853, x1000) secondary antibodies overnight at 4°C in TBST. The next day membrane was washed three times 5 min in TBST, then incubated in HRP-conjugated secondary antibodies (anti-mouse IgG, NA9310, x 50,000; anti-rabbit IgG, NA9340, x50,000) for 1 hour at RT in TBST. The membrane was washed three times 5 min at RT in TBST. Bands were visualised using ECL prime chemiluminescent reagent (GE Healthcare) following manufacturer's instructions in a Fujifilm Las-4000 imager (Fuji, Japan).

Supplemental Figure 1. *Bmal1*$^{L-/-}$ mice have disrupted circadian clock in the liver, related to Figure 1. Clock gene expression analysis in the liver of WT and *Bmal1*$^{L-/-}$ mice kept in constant darkness. Real-time PCR with a primer pair targeted to the deleted *Bmal1* region (exon 6 to 8) did not lead to any significant amplification; the circadian clock in the liver has efficiently been disrupted. This is confirmed with the expression of the canonical clock genes *Per1* and *Per2* in the liver of the same animals, showing severely blunted expression. All data are mean +/- SEM, n = 3. The frame on top of each graph indicate significance level of gene expression in wild-type animals in one-way ANOVA (top), followed underneath by the comparison of gene expression between WT and *Bmal1*$^{L-/-}$ animals by Two-way ANOVA (Interaction/Time/Genotype).

Supplemental Figure 2. Genes involved in the synthesis and supply of nucleotides are strongly expressed in the liver, related to Figure 1. (A), The liver is the main supplier of nucleoside and bases to other tissues throughout the body. In agreement to that, expression of *Pnp*, *Upp2* and *Tymp*, encoding nucleoside phosphorylases, is dramatically higher in the liver compared to the adrenal gland or to muscle tissue. **(B)**, *Rrm2* expression is rhythmic and in limiting amount compared to the *Rrm1* subunit (left), consistent with RRM2 as the rate-limiting subunit of the whole RRM enzyme. *Upp2* expression in the liver is 100-fold higher than that of *Upp1* (right), indicating that *Upp2* encodes the main uridine phosphorylase activity detected from the liver.

Supplemental Figure 3. Mean abundance of purine and pyrimidine in the liver, related to Figure 2. (A), Mean abundance of purine bases, nucleosides and nucleotides. **(B)**, Mean abundance of pyrimidine bases, nucleosides and nucleotides.

Supplemental Figure 4. Variations in AK2 protein quantity in the WT liver across a day in constant darkness, related to Figure 1. AK2 (lower bands at 26 KDa) and β-Actin (upper bands at 42 KDa) proteins were visualised on the same membrane using different primary and secondary antibodies. n = 2 animals per time point, their corresponding sample loaded sequentially in two CT0-20 series. Note the higher intensity of bands at CT12-20.

Supplemental Table 1

Sequence of primers used for quantitative real-time PCR		
Target gene	**Sense primer (5'-3')**	**Antisense primer (5'-3')**
Ak2	GGAGGATCACTGGGAGGCTGAT	CGTTGTCATCTGACCTGCGGA
Ak4	GGGAGGGTCTATAACCTGGAC	TCCTTGTACCGTCTTAGCCTG
Bmal1	AGGCGTCGGGACAAAATGAACA	TGGGTTGGTGGCACCTCTCA
Cad	AGAAAGGGACAGAGCCGTCAG	ATCCAGAGCACAGATCCGAGG
Cmpk2	CTGCTTAACTCTGCGGTGTTC	CTTTCTGGACCTCCTTTGGGC
Ctps	GGAAGACTGTCCAGGTTGTCCC	AATGTCTCCCACTGTGCCACC
Ctps2	AGCCAGTCACCAAAGCCGAGGA	CCTTGCCCACGAAATTGCCTG
Dpyd	CCACCGCAGCCAAGAAACTAG	TCGCTCACCAAGAGTCGTGTG
Per1	TGGCTCAAGTGGCAATGAGTC	GGCTCGAGCTGACTGTTCACT
Per2	CCATCCACAAGAAGATCCTAC	GCTCCACGGGTTGATGAAGC
Pnp	TTAGGAGGGCTGACTGCTCAC	GCATCATCACACAGGATCTGC
Ppat	GGGTATTGGGCTTTCCACGTC	TAACCAGGGAGTATGCTGCGG
Rrm1	CACCCTGACTATGCCATCCTGG	GAGAGTGTCTGCCGTTGTGCG
Rrm2	CTGTTTCTATGGCTTCCAAAT	TTCTTCTTCACACAAGGCATT
Tk1	CGGAGAGTGTGGTGAAGCTCA	CACGGAGTGATACTTGTCGGC
Tk2	TCCAAGACCCCATCACTCTCTC	TGACTTCTTCATGCTCGTGGTC
Tymp	AGGTCCCTTCACCCTTCGCTGA	CCTAGAGCCAGTAGCATCGTG
Umps	GGCGACAGTTATCTGCTCAGC	CGTCCTCAATGACCAGACAGG
Upp1	CCTCAGCACTAGCACACACGA	GGATATTCCTTCCCTGGATGG
Upp2	CGGTTGGAGGGAGATGGAGAA	AATGGAAATGGAGGGGATGCC

Supplemental table 1 Sequences of oligonucleotide primers used in qPCR in Figure 1.

Supplemental References

Soga, T., and Heiger, D.N. (2000). Amino acid analysis by capillary electrophoresis electrospray ionization mass spectrometry. Anal. Chem. *72*, 1236-1241.

Soga, T., Ishikawa, T., Igarashi, S., Sugawara, K., Kakazu, Y., and Tomita, M. (2007). Analysis of nucleotides by pressure-assisted capillary electrophoresis-mass spectrometry using silanol mask technique. J. Chromatogr. A *1159*, 125-133.

Sugimoto, M., Wong, D.T., Hirayama, A., Soga, T., and Tomita, M. (2010). Capillary electrophoresis mass spectrometry-based saliva metabolomics identified oral, breast and pancreatic cancer-specific profiles. Metabolomics *6*, 78-95.

Supplemental Figure 1

Click here to download high resolution image

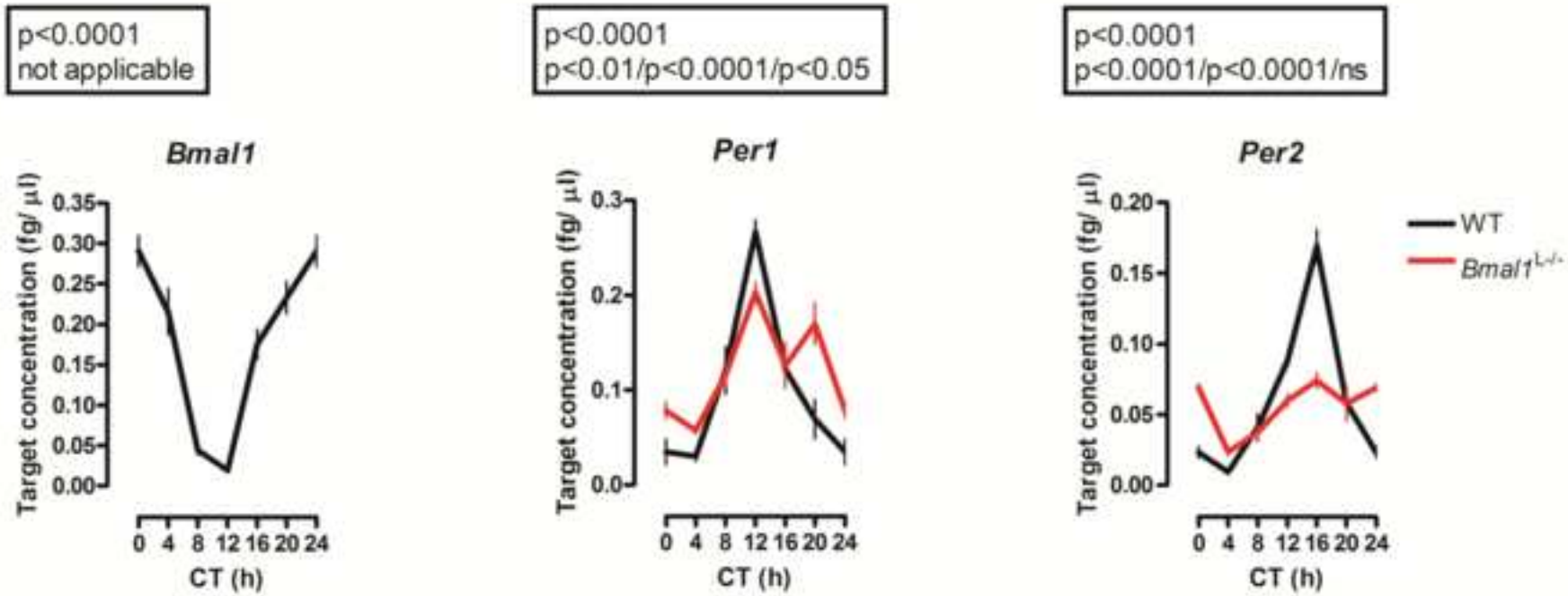

Supplemental Figure 2

Click here to download high resolution image

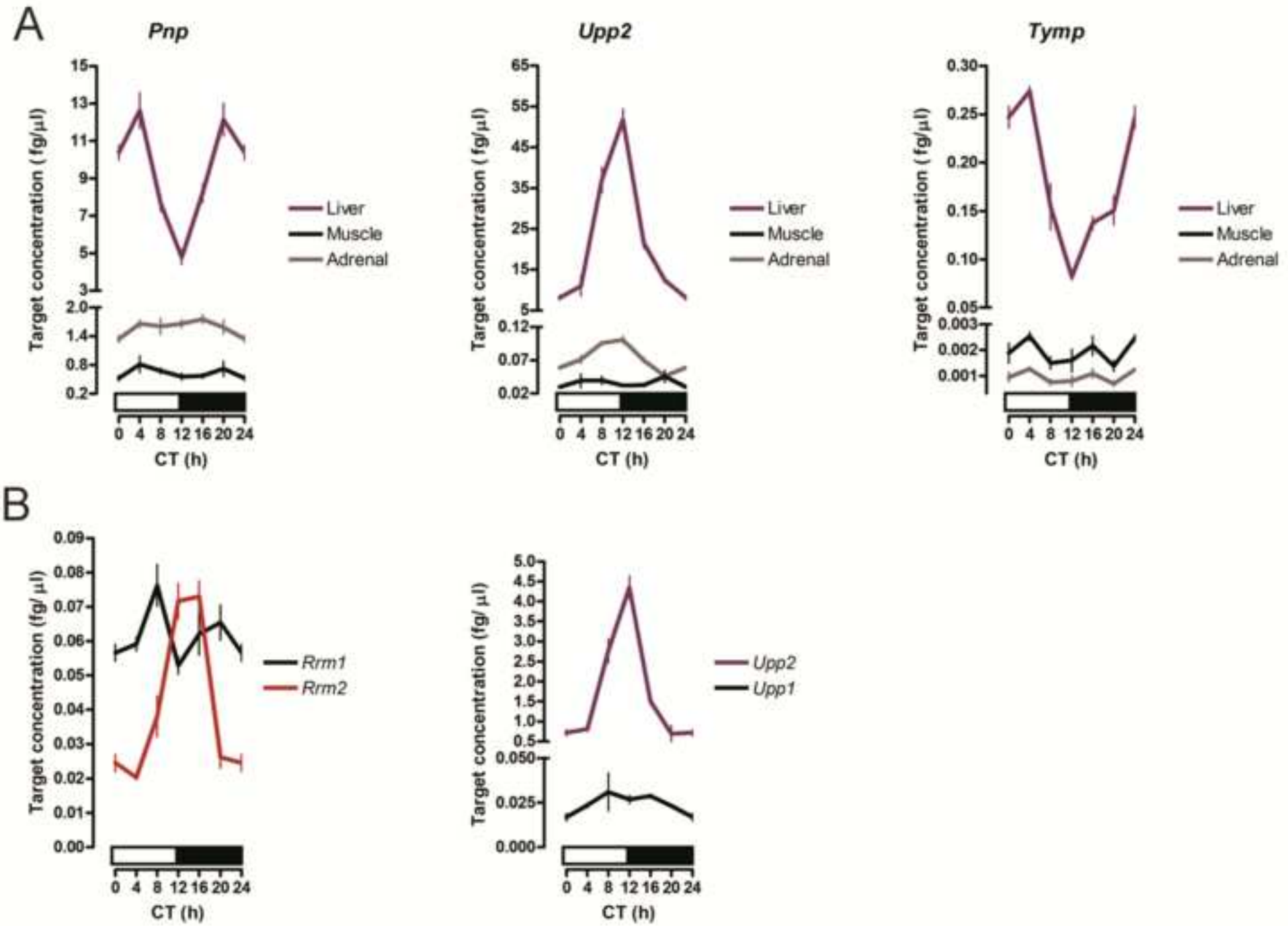

Supplemental Figure 3
Click here to download high resolution image

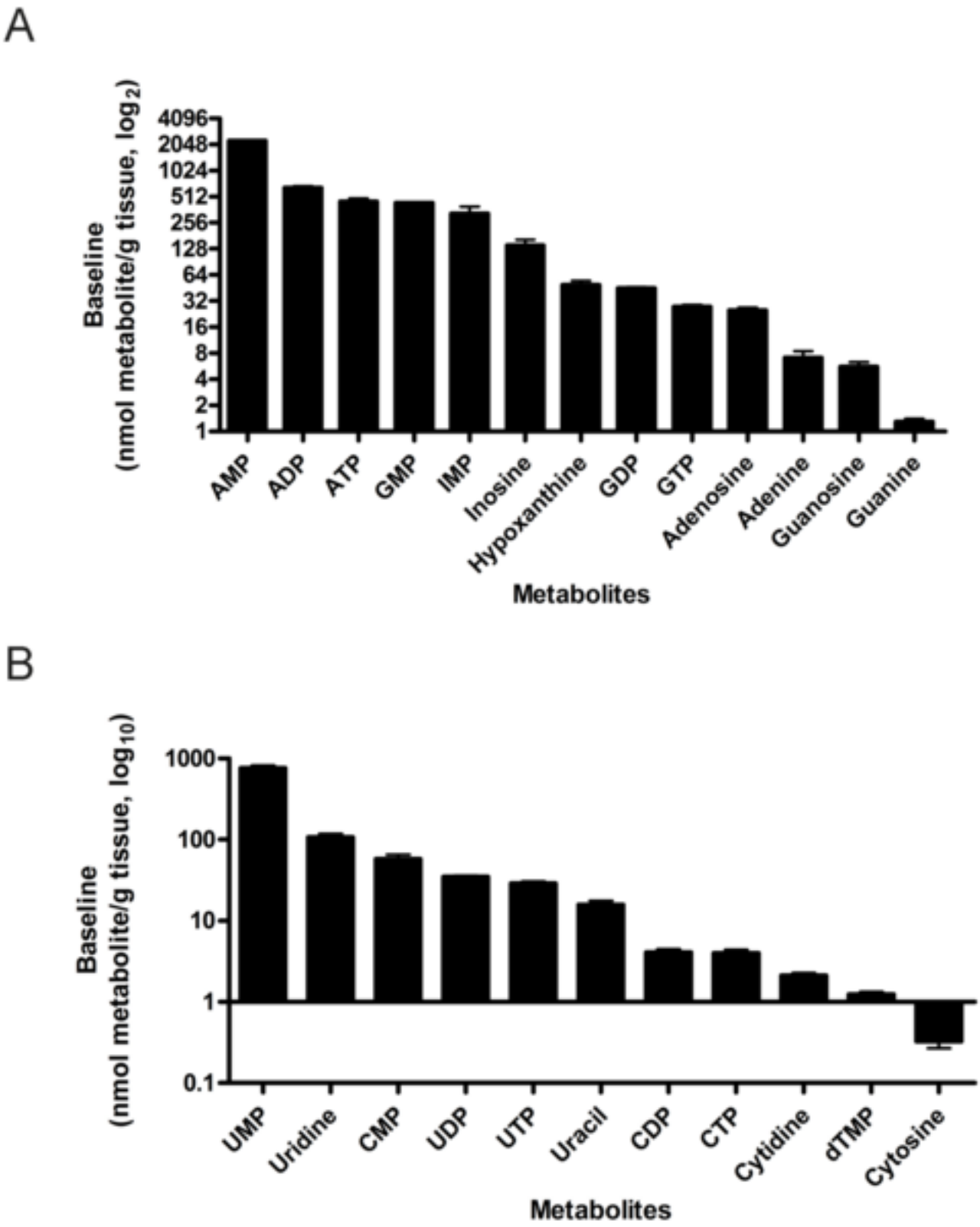

Supplemental Figure 4

Click here to download high resolution image